SAND2007-5209C

Pull Strength Evaluation of Sn-Pb Solder Joints Made to Au-Pt-Pd Conductor on Low-Temperature Co-Fired Ceramic[1]

P. Vianco, F. Uribe, and G. Zender
Sandia National Laboratories
P.O. Box 5800 MS0889, Albuquerque, NM 87185
ptvianc@sandia.gov

Abstract

Cracking was observed in the side walls of gold (Au) filled vias in low-temperature, co-fired ceramic (LTCC) substrates. Further analysis indicated the likely source as the constituents of the glassy phase component of the gold-platinum-palladium (Au-Pt-Pd) thick film used for the conductor layers. The successful approach toward mitigating the cracking phenomenon was to place a barrier Au thick film layer between the Au-Pt-Pd layer and the LTCC substrate that significantly curtailed the diffusion of glassy phase components from the former, into the latter. However, it was necessary to determine the effects of the additional thick film layer on the microstructure and overall mechanical strength of tin-lead (Sn-Pb) solder joints made to these pad structures. Acceptable pull strengths were measured in the range of 3.5 – 4.0 lbs. The solder joint pull strength was sensitive to the number of firing steps as defined by the thick film layer construction. Both the solder/thick film and thick film/LTCC interface strengths had roles in this trend, thereby affirming the synergism between material, interfaces, and the firing processes The pull strength was optimized when the pad length ratio, 4596:5742, was 1.0:0.5, which was characterized by a reduced occurrence of the thick film/LTCC failure mode.

Introduction

A contributing factor to the long-term reliability of hybrid microcircuit (HMC) assemblies is the integrity of the soldered interconnections. Hybrid microcircuit assemblies use ceramic base materials in place of the traditional, organic laminate-based, printed circuit boards. Instead of a built-up copper (Cu) layer providing the conductive traces and solder bond pads, thick film or thin film layers are used to create these features. Thick films are comprised of the elemental metals, or alloy combinations of, Au, silver (Ag), Pt, and Pd. These compositions are readily solderable by tin (Sn)- and indium (In)-based alloys. The addition of the higher melting temperature Pt and Pd metals reduces dissolution of the layer by molten solder. Textbooks by Harper as well as by Holmes and Loasby provide excellent review discussions of HMCs and detailed accounts of thick film technology [1, 2].

The pattern of thick film conductor traces and pads is created by screen printing the thick film *ink* on the ceramic substrate. The ink is comprised of the metal particles, a glassy phase, and the organic (rheological) components. A drying step removes the volatile organic constituents. Then, the firing step (850°C, 5 – 20 min) volatizes the remaining organic components and causes the metal particles to sinter together. The degree of sintering is often incomplete, leaving the metal layer with various degrees of porosity. The metal component adheres to the ceramic by the migration of the glassy phase to the metal/ceramic interface. The glassy phase bonds the metal component to the ceramic substrate. The bond pad thickness can be increased by performing multiple print-dry-fire sequences. Thick film layers range from approximately 8 μm for a single layer to 20 μm thick for a triple thick layer.

The mechanical strength of solder joints made to thick film bond pads is a function of the strengths of the three constituent materials: the solder, the thick film, and the substrate, as well as depends upon the adhesion strength of the solder/thick film and thick film/substrate interfaces. The solder/thick film interface is characterized by an intermetallic compound (IMC) layer; the thick film/ceramic interface is comprised of the glassy phase. Numerous studies have examined the strengths of thick film pads, either by themselves or the component of a solder interconnection, as a function of firing parameters, print thickness, alloy composition, etc. [3 – 5]. Historically, thick film adhesion studies have addressed primarily oxide substrates (alumina, beryllia, etc.). There have been fewer, detailed studies of the strength and microstructures of thick film layers on low-temperature, co-fired ceramic (LTCC) substrates.

A development effort at Sandia, which evaluated Au-Pt-Pd thick film on LTCC, resulted in a finding of cracks in the walls of Au-filled vias under bond pads formed from a Au-Pt-Pd thick film (Fig. 1). Besides potentially weakening the LTCC material under the interconnection, the via cracks could also sever internal traces within the substrate structure, leading to an electrical failure. A materials analysis identified elevated concentrations of Bi to be associated with the cracked regions, which indicated that the Au-Pt-Pd glassy phase had diffused into the region [6]. Residual stresses provided the driving force for crack initiation and propagation. The mitigation strategy was to identify a thick film composition, which could be placed between the Au-Pt-Pd layer and LTCC substrate that would serve as a barrier to the diffusion of glassy phase material. A candidate barrier layer thick film was identified and did successfully prevent the formation of via cracks. Next, it was necessary to determine the effects of the barrier layer footprint on the pull strength and microstructure of solder joints made to such pads. The results of that study are reported below.

[1] Sandia is a multiprogram laboratory operated by Sandia Corporation, a Lockheed Martin Company, for the US Dept. of Energy's National Nuclear Security Administration under contract DE-AC04-94AL85000. *The use of product identification numbers is for brevity purposes, only, and does not indicate an endorsement of any one supplier.*

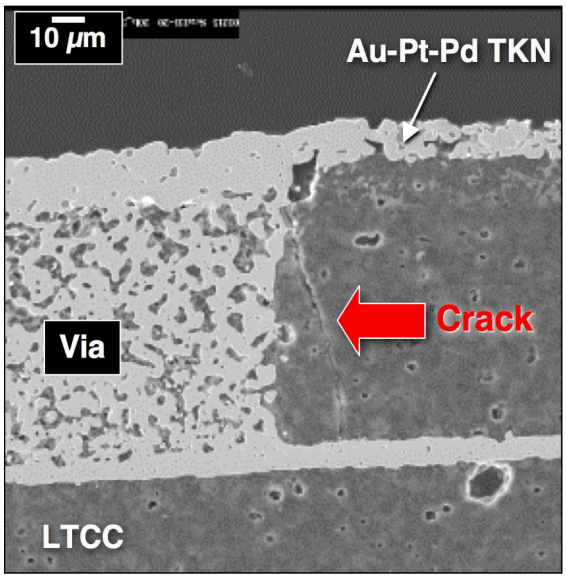

Fig. 1 SEM/SE image of a crack in the sidewall.

Experimental Procedures

The LTCC test vehicles were built from DuPont™ 951AX green tape (four layers) [7]. A schematic diagram of the test vehicle is shown in Fig. 2a. The substrate measured 1.0 x 1.0 x 0.036 in. After the green tape layers were pressed and fired ("processed"), a pattern of nine (9) thick film solder pad structures was "post-processed" on one surface. The square pad structures were constructed of combinations of the Au-Pt-Pd DuPont™4596 thick film (abbreviated 4596) and Au DuPont™5742 thick film (abbreviated 5742). The thick film structures for cases with and without vias are shown in Fig. 2b. The triple-thick 4596 layer was fabricated from three sequential print-dry-fire processes. Only a single layer of 5742 thick film was evaluated. In the absence of vias, the same footprint area was used for both the 4596 and 5742 layers (Fig. 2b). When vias were present, different 5742 layer footprints were evaluated that were identified by the ratio of the x dimensions between the two layers (white arrows in Fig. 2c). The vias were filled with the Au-based, DuPont™5738 material. Three vias were located under a bond pad, having been arranged in a triangular pattern about the center.

The matrix of thick film layers to which, the solder joints were made, is listed below:

1. 1x 4596; no vias
2. 3x 4596; no vias
3. 1x 5742, 1x 4596; no vias
4. 1x 5742, 3x 4596; no vias

5. 1x 4596; vias
6. 1x 5742; vias

7. 1x 5742, 1x 4596, [1.0:1.0]; vias
8. 1x 5742, 1x 4596, [1.0:0.5]; vias
9. 1x 5742, 1x 4596, [1.0:0.2]; vias
10. 1x 5742, 3x 4596, [1.0:1.0]; vias
11. 1x 5742, 3x 4596, [1.0:0.5]; vias
12. 1x 5742, 3x 4596, [1.0:0.2]; vias

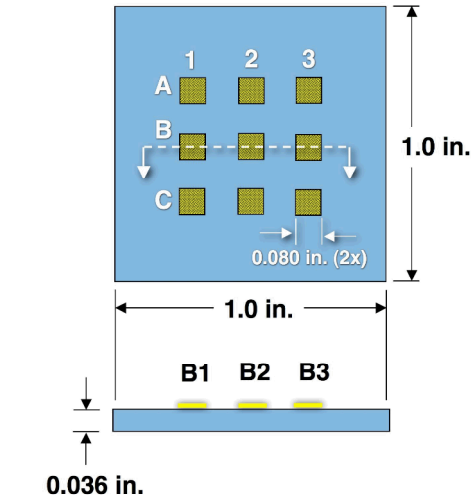

(a)

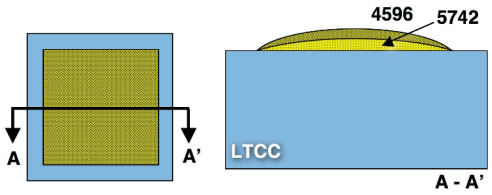

(b)

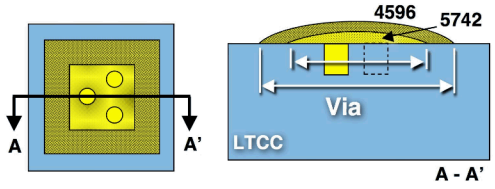

(c)

Fig. 2 (a) Schematic diagram of the test vehicle. (b, c) Schematic diagrams showing the thick film layer constructions both with and without vias.

The symbols "1x" and "3x" indicate single layer and triple 4596 layers, respectively. The ratios – e.g., [1.0:0.5], is that of the 4596 length dimension to the 5742 length dimension (Fig 2c).

The first grouping numbered 1 – 4 established the baseline strength performances, not only for this study, but to also compare with historical data. The samples 5 and 6 determine the effect of via cracks on the solder joint strengths. The groupings 7 – 9 and 10 – 12 evaluate the geometry of the

5742 barrier layer with thin (1x) and thicker (3x) 4596 layers, respectively.

The pull strength was evaluated for solder joints that were made to the thick film sites, using the so-called "DuPont pull test" or "shepard's hook pull test". The 63Sn-37Pb (wt.%) alloy (Sn-Pb) was used to make all joints except those made directly to the 5742 layer (case 6 above). In that latter instance, the 50In-50Pb (In-Pb) solder was used to prevent excessive leaching of the pure Au thick film composition. Tin-coated Cu wires were attached to the thick film pads using a Sn-Pb immersion process (260°C, 5 s). In the case of the In-Pb solder, Au-Ni plated Cu wires were used; the solder bath parameters were the same. A test sample is shown in Fig. 3a prior to forming and pull testing. The "shepard's hook" end on the right was clipped off; then, both ends were formed upwards. The test sample was placed in a servohydraulic test frame with the substrate secured into place and the cross head attached to an upright length of wire. Only the outboard joints A1, A3, B1, B3, C1, and C3 were pull tested (Fig. 3b); the center joints were used for (as-fabricated) microstructure analysis. The pull tests were performed at a crosshead speed of 12 mm/min. The maximum load was recorded from each test.

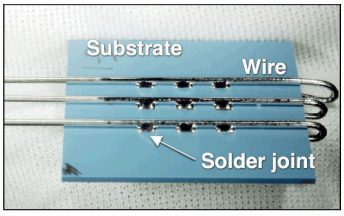

(a)

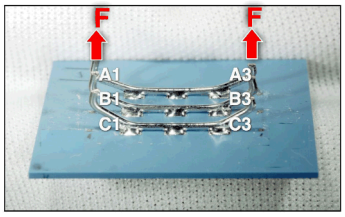

(b)

Fig. 3 Stereo photographs of the test vehicle: (a) after solder attachment of the wires and (b) following pull testing of the outboard joints A1, A3, B1, B3, C1, and C3.

Three (3) substrates were tested per thick film condition (1 – 12), resulting in a total of 18 values for each case. The maximum load values were combined and represented as a mean and an error term of ±95% confidence interval (about the mean).

Failure mode analysis was performed by visual inspection as well as using metallographic cross sections of the pull-tested joints. For brevity, only the quantitative data from the visual inspections will be discussed here. The results from metallographic cross sections will be limited to qualitative trends. The four failure modes that were used in the visual inspection are described in Fig. 4. The modes #1 and #2 were distinguished by the completeness of the separation along the solder/thick film (abbreviated TKN) interface. Mode #3 was failure within the solder. Failure mode #4 was primarily separation at the thick film/LTCC interface, but could have included, as well, a divot of LTCC material from the substrate below it.

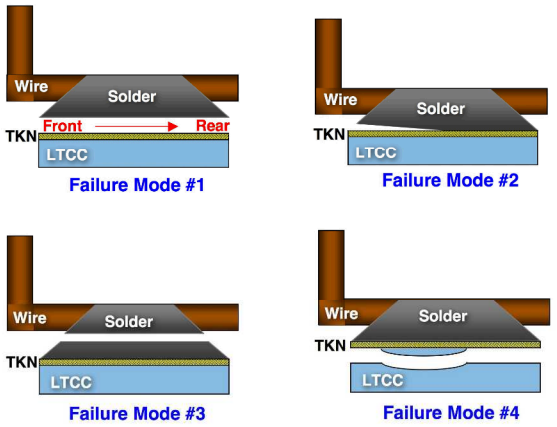

Fig. 4 Failure modes: #1 complete solder/thick film (TKN) separation; #2 partial solder/TKN separation; #3 solder failure; and #4 TKN/LTCC with LTCC divot, if present.

An accounting of the visual inspection failure modes was performed in the following manner. Each of the four failure modes was either present (1) or absent (0) at the test site. Then, the percentage of the eighteen pull test sites having each of the four failure modes was calculated. Since the failure mode percentages were not mutually exclusive, the total per condition did not necessarily equal to 100%.

Results and Discussion - Microstructures

The microstructures were examined that represented the as-fabricated joints. Shown in Fig. 5 are scanning electron microscope (SEM) photographs of the solder joint made to the 1x 4596 thick film layer. The low magnification image in Fig. 5a shows the entire solder joint. The voids were not unexpected for this geometry and assembly process. Also, the extent of voiding would not significantly impact the strength performance of the solder joint. The SEM photograph in Fig. 5b shows the interface microstructure. The thick film layer is 8 – 10 µm thick. The shadow in the solder field is due to preferential polishing of the Sn-Pb solder. The IMC layer is very thin at the solder/thick film interface in the as-fabricated conditions of all samples.

Of particular interest was the glassy phase identified in Fig. 5b. Electron probe microanalysis (EPMA) showed that phase to be high in Bi and cadmium (Cd), indicating that its source was the 4596 thick film layer. Neither Bi nor Cd are present in the LTCC material, which is comprised of silica (SiO_2), alumina (Al_2O_3), and a Pb-based glassy phase (likely Pb_2O_3). It was interesting to note from the EPMA that the Bi-rich component diffused to only within the first 1 – 2 LTCC grains from the interface. On the other hand, the Cd diffused nearly 7 – 8 grains into the LTCC at which point, the EPMA trace ended. The Cd-rich material likely traveled further because there was no evidence that the Cd concentration had a

decreasing gradient at the end of the trace. The Cd content of the thick film was almost completely depleted by this diffusion activity. A similar analysis was performed on the 3x 4596 thick film specimen. Except for the thicker layer (15 – 20 µm), the microstructures were similar to those in Fig. 5 and the EPMA data exhibited similar behaviors of Bi and Cd components of the Au-Pt-Pd thick film glassy phase.

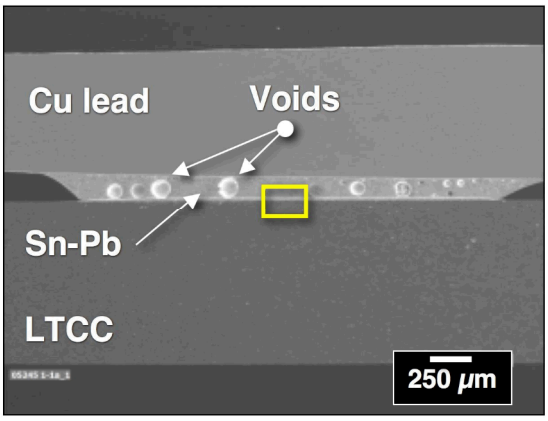

(a)

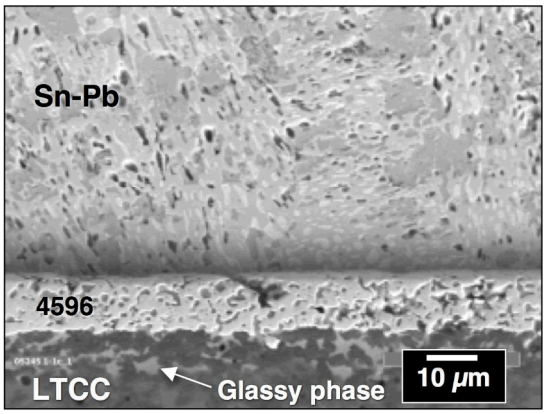

(b)

Fig. 5 SEM photographs of the cross section of the as-fabricated Sn-Pb solder joint made to the 1x 4596 thick film: (a) low magnification image of the entire joint and (b) high magnification of the solder/thick film/LTCC structure.

The In-Pb solder joints were made to the 1x 5742 layer. An SEM image of the as-fabricated interconnection is shown in Fig. 6. The 1x 5742 layer is approximately 8 – 10 µm thick. There are three points of particular interest: (a) The EPMA indicated the layer to be nearly 100% Au and no detection of a glassy phase. (b) The layer was nearly fully dense. The higher density results from the improved sintering capabilities of pure Au in the absence of Pt, which has a considerably higher melting temperature. (c) There was no accumulation of a glassy phase at the thick film/LTCC interface nor in the LTCC material. The joint had excellent integrity.

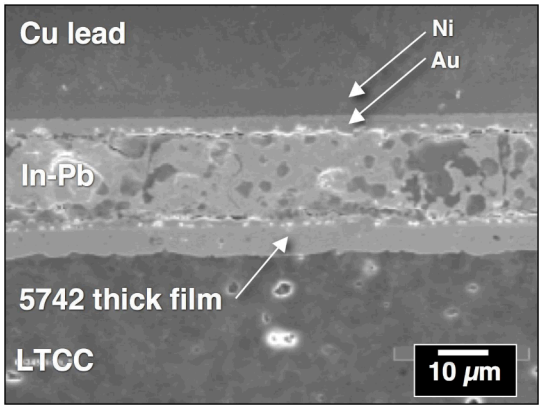

Fig. 6 SEM photograph showing the In-Pb solder joint made to the Au-Ni plated Cu wire and the 1x 5742 thick film (barrier) layer.

The thick film was examined, which was a combination of the 1x 5742 and 1x 4596 layers, representing the as-fabricated condition. An SEM image of the associated Sn-Pb solder joint is shown in Fig. 7. There were no indications of cracking or delamination between any of the materials. A string of small pores provided an apparent demarcation between the two thick film layers, based upon expected thicknesses. There were small, isolated regions of 4596 glassy phase that had infiltrated into the LTCC substrate, along the thick film/LTCC interface (not shown in Fig. 7). But, these infiltrations occurred to a considerably lesser degree than was observed with the 1x 4596 layer (Fig. 5b).

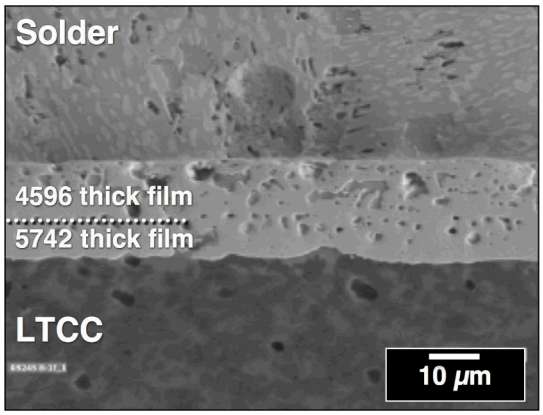

Fig. 7 SEM photograph showing the Sn-Pb solder joint made to layer built up with 1x 4596 and 1x5742 thick films.

The EPMA technique was used to assess the distribution of elements across the 1 x 5742, 1x 4596 thick film structure. A representative trace is shown in Fig. 8. Primarily, it is the Au concentration that delineates the 5742 layer from the 4596 layer. There was a noticeably diffusion of Pt and, to a lesser extent, Pd, from the 4596 layer into the 5742 barrier layer. The Pt and Pd diffusions were likely supported by the extensive mutual solubility between those elements and Au.

Most importantly, however, was the fact that the Cd and Bi glassy phase components remained in the 4596 layer.

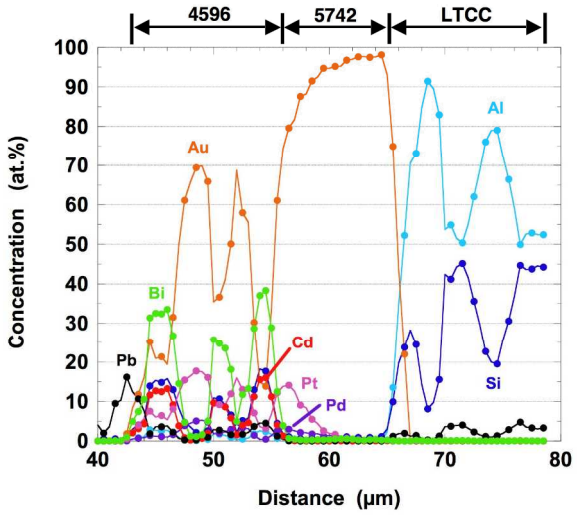

Fig. 8 EPMA graph showing the elemental distribution across the composite 1x 4596, 1x5742 thick film structure.

A comparison was made between the SEM image in Fig. 7 and EPMA trace in Fig. 8. An overlay of the microstructure and Au profile indicated that, what appeared to be pores that demarked the 5742 and 4596 layers, were actually an accumulation of the Bi- and Cd-rich glassy phase particles from the 4596 layer. The glassy phase accumulated to a greater extent along the boundary between the 1x 5742 layer and 3x 4596 layers (Fig. 9) due to a greater quantity of glassy phase and two additional firing steps. Therefore, the driving force persisted for the glassy phase of the 4596 layer to reach the LTCC substrate despite the presence (and successful intervention) of the 5742 layer.

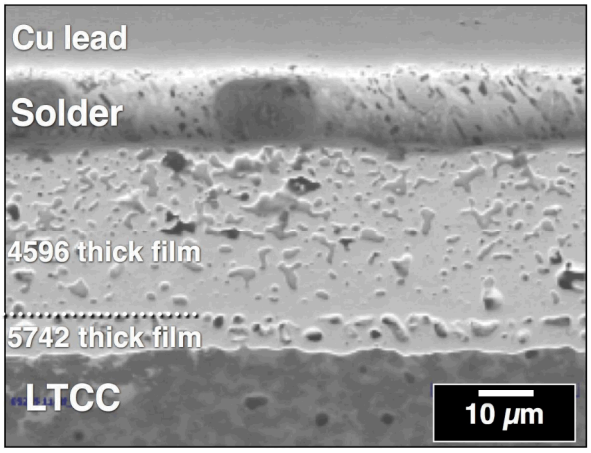

Fig. 9 SEM photograph of the thick film layer comprised of the 3x 4596 layer over a 1x5742 layer.

The SEM analysis and EPMA data identified two other differences between the 3x 4596 layer versus the 1x 4596 layer structures having the 1x 5742 barrier layer. First, there was a greater extent of Pt and Pd diffusion into the 5742 layer in the 3x 4596 case, which was a result of the additional firing steps. Second, there was a greater frequency of breaches of the 5742 layer by the 4596 glassy phase as indicated by the diffusion of Bi and Cd into isolated regions of the LTCC substrate. Fortunately, the extent of diffusion by either element was limited to approximately 1 – 2 grains from the thick film (5741)/LTCC interface.

The following remarks summarize the microstructural observations that were made when vias were added to the solder joint structure. In case 5 for which, a 1x 4596 layer, is placed over a via, side wall cracks appeared adjacent to the via, as expected. On the other hand, when the 1x 5742 layer was placed between the LTCC substrate and either the 1x or 3x 4596 layer thicknesses and LTCC substrate, cracks were not observed in nearby vias. The introduction of the 1x 5742 thick film did not cause observable degradation to the pad, LTCC, or solder joint structures. Also, there was no correlation between solder joint void propensity and/or location as a function of thick film structure or the location of the via under the pad.

The microstructures were similarly examined, which belonged to the combined 5742 and 4596 layers, but having the 1x 5742 footprint with a length dimension less than that of the 4596 layer. Of particular interest was the microstructure at the edge of the 5742 layer and, specifically, the extent of lateral diffusion by the 4596 glassy phase components. Shown in Figs 10 and 11 are the cases for the 1x 4596 and 3x 4596 layers, respectively. The length ratio was 1.0:0.5. The 4596 glassy phase diffused laterally by a distance of approximately 20 µm under the 5742 layer with the single firing step of the 1x 4596 layer. However, the three firing steps of the 3x 4596 layer resulted in a lateral diffusion of nearly 43 µm by the glassy phase under the 5742 layer. It was also interesting to note in Fig. 11 that the more extensive presence of Bi and Cd glassy phase constituents in the LTCC substrate resulting from the 3x 4596 layer, exhibited both fine and coarse morphologies.

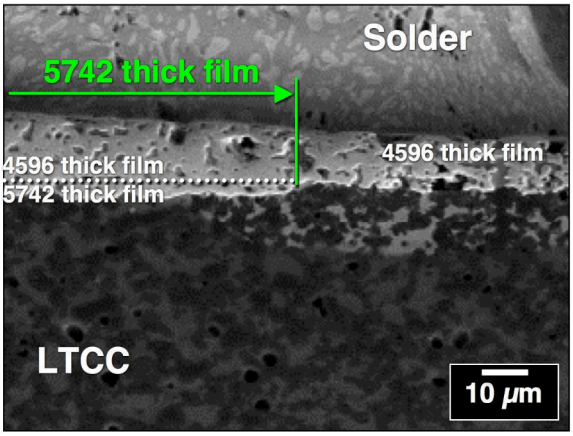

Fig. 10 SEM showing the edge of the 1x 5742 layer under the 1x 4596 layer and the extent of 4596 glassy phase lateral diffusion. The length dimension ratio was 1.0:0.5.

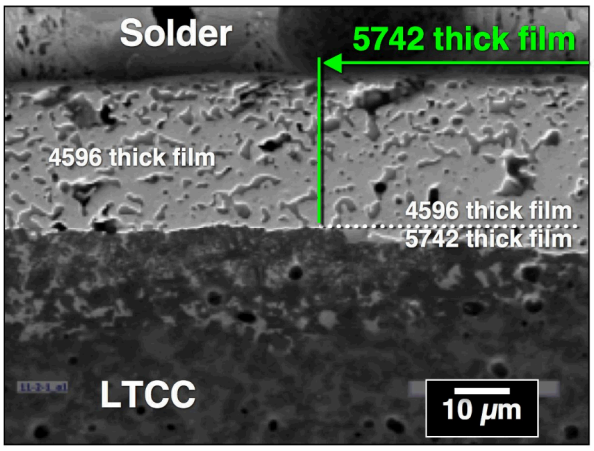

Fig. 11 SEM showing the edge of the 1x 5742 layer under the 3x 4596 layer and the extent of 4596 glassy phase lateral diffusion. The length dimension ratio was 1.0:0.5.

The latter, only, characterize the 1x 4596 case (Fig. 10). Lastly, in spite of the lateral diffusion, which in the worst case of geometry and processing, allowed the Bi- and Cd-components of the glassy phase to approach a via to within 63 µm, cracks were not observed in the side walls.

In summary, the microstructural analysis indicated that the introduction of the 1x 5742 layer between the LTCC substrate and either 1x or 3x 4596 thick film layers eliminated via side wall cracking in *all* cases. The 5742 layer provided a satisfactory barrier against the diffusion of Bi- and Cd-based glassy phase components from the 4596 thick film as determined by EPMA. The overall integrity of the solder joint structures was excellent.

Results and Discussion – Mechanical Testing

The solder joint pull strength data were compiled in Fig. 12; the error bars represent the 95% confidence interval about the mean. The background colors identify test specimen structures having related features. The strengths of the 1x and 3x 4596 thick film solder joints (without vias and without the 5742 layer) were compared to historical strength data obtained from Sn-Pb solder/4596 thick film interconnections on alumina substrates (no vias). The current pull strengths were slightly less than those prior data (4.3±0.87 lb) although still well within acceptable performance criteria [8]. Interestingly, the scatter was considerably lower in the present results.

The specific observations that were made from Fig. 12 were as follows:

(a) In the absence of vias, the mean strength of the 3x 4596 thick film was slightly higher than that of the 1x 4596 layer (green background); however, statistically, there was no significant difference between the two values.

(b) The addition of the 1x 5742 layer to the 1x 4596 layer (blue background, no vias) resulted in a significant increase of pull strength. However, the addition of the 1x 5742 layer to the 3x 4596 layer did not produce the same strength increase; instead, the values remained similar to those of the 3x 4596 layer, alone.

(c) The placement of vias under the 1x 4596 layer did not alter the solder joint pull strength. This observation was of particular interest because it indicated that the pull strength was not sensitive to side wall cracks in the vias. (Thus, side wall cracks pose more of an electrical reliability concern – that is, severing of internal traces – than a concern of pull strength degradation.)

(d) The pull strength of the In-Pb solder joint made to the 1x 5742 layer over a via (yellow background) was similar to that of the 1x 4596 layer (with or without a via). Therefore, the 5742/LTCC interface was at least as strong as the 4596/LTCC interface.

(e) The 1x 5742, 1x 4596 and 1x 5742, 3x 4596 configurations, having the 1.0:1.0 footprint and vias under the thick film layers (purple and pink backgrounds, respectively), exhibited statistically similar pull strengths. While the strength of the latter layer configuration was comparable to that of the "no via" case, in the former case, the addition of the via resulted in a loss of the strength "advantage" realized with the 1x 5742, 1x 4596 layer case.

(f) Three trends were observed with respect to the effect of layer footprint length distance ratio on the *mean* pull strength. The strength differences all remained within the statistical error. First, the strengths of the thick film structures having the 3x 4596 layer were slightly lower than those having the 1x 4596 layer. Second, the maximum strength occurred with the 1.0:0.5 distance ratio for both 1x and 3x 4596 layer thicknesses. Third, the data scatter was least for the 1.0:1.0 ratio value.

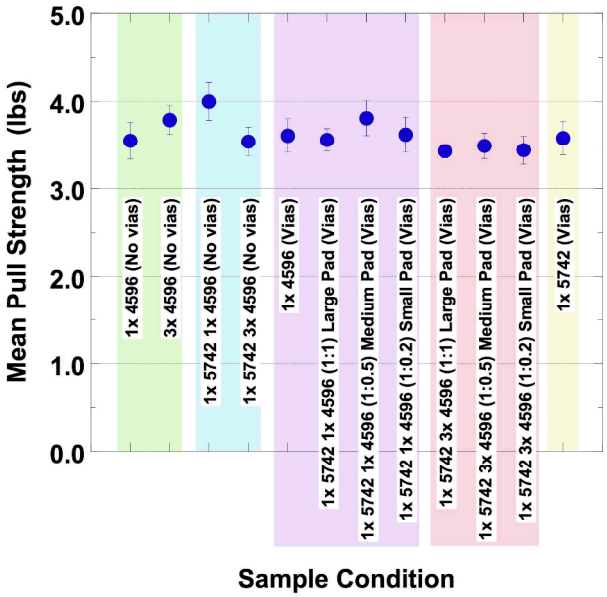

Fig. 12 Pull strength as a function of thick film configuration. The scatter is ±95% confidence interval.

The results of the failure analysis by visual inspection are shown in Fig. 13; refer to Fig. 4 for illustrations of each of the failure mode. The failure mode observations will be discussed in conjunction with the pull strength trends in Fig.

12. The "no via" data can be compared directly to the corresponding "via" data by means of the 1.0:1.0 ratio samples. Lastly, the discussion will address failure modes #1, #3, and #4 since these modes were sensitive to the specimen pedigree. The failure mode #2 was recorded on all of the samples.

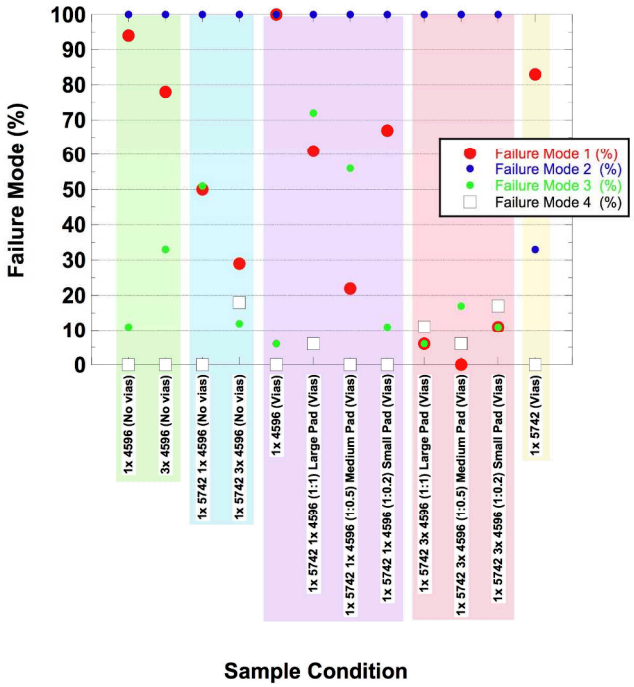

Fig. 13 Failure mode analysis based upon visual inspection.

The test cases that will be evaluated first were those that did not have vias (green background in Fig. 13). The slightly higher strength of the Sn-Pb solder joints having only the 3x 4596 layer versus the 1x 4596 layer (Fig. 12) was due to a slightly stronger solder/thick film interface as evidenced by the drop in the failure mode #1 (green background). The decrease of the mode #1 was compensated by an increase of fracture in the solder (#3). A similar trend accounted for the large strength increase observed when the 1x 5742 layer was introduced between the 1x 4596 layer and LTCC substrate (blue background). However, when the 1x 5742 layer was introduced underneath the 3x 4596 layer, the reduced pull strength (vis-à-vis the former case) was accompanied by an increased occurrence of the #4 failure mode. The latter trend implied that there was a weakening of the thick film/LTCC interface.

Next, the effects of vias were considered (1.0:1.0 ratio, purple and pink backgrounds). In the direct comparisons between 1x 4596 samples with and without vias, the failure modes were similar, which corroborated the pull strength data that indicated that side wall cracks did not affect the mechanical performance of the solder joint.

The addition of the via caused the strength of the 1x 5742, 1x 4596 samples to decrease to a level that was more similar to the other test cases. All failure modes were higher for the samples having a via (1.0:1.0, purple background), including the small contribution by the #4 failure mode. This trend suggests that the structural discontinuity resulting from the via can affect mechanical properties of the solder joint, but more so the strength than failure mode because the strength was so very high.

The samples having 1x 5742 and 3x 4596 layers exhibited little sensitivity of the pull strength to the presence of the vias. The addition of the via caused slight decreases in all of the #1, #3, and #4 failure modes (1.0:1.0, pink background) versus the case without a via. An increase of failure mode #2 compensated for the reduced frequencies of the other modes.

Lastly, the In-Pb solder joints made to the 1x 5742 layer (with vias) showed a failure mode behavior (yellow background) that was similar to that of the 1x 4596 layer, with or without vias. The predominant failure mode was solder/thick film separation. This similarity extended to the pull strength data (Fig. 12). Therefore, there is no evidence that the addition of the 5742 layer would degrade the interconnections, either through its intrinsic strength or it adhesion to the LTCC substrate.

An evaluation was made of the effect of the length distance ratio between the 4596 layer and 5742 layer footprints. Recall that these samples had vias. First of all, an overall comparison between the cases having a 1x 4596 layer (purple background) versus those with the 3x 4596 layer (pink background) indicated a lesser presence of the thick film/LTCC failure mode #4 and greater contributions by the #1 and #3 failure modes in the 1x 4596 case. Recall that these samples also experienced slightly higher pull strengths, as well.

Whether there was a 1x or 3x 4596 layer present, both cases showed a similar dependence of failure mode on ratio. The #1 and #4 failure modes were minimized with the 1.0:0.5 ratio, which also exhibited the maxima in the pull strength values for both groups.

The analysis of the failure modes (Fig. 13), together with the pull strength data (Fig. 12) indicated the following trends: (a) The presence of the 1x 5742 layer did not intrinsically degrade the pull strength of the solder joints. (b) Increasing the number of 4596 layers in the presence of the 1x 5742 layer (with or without vias) resulted in lower mean pull strengths and increased propensity for failure at the thick film/LTCC interface (often accompanied with an LTCC divot). (c) Consistent trends were observed in both pull strength and failure mode as a function of pad length distance ratio. Maximum strength was accompanied by minimizing, foremost, the thick film/LTCC failure mode #4 and then, secondarily, minimizing fracture at the solder/thick film interface (modes #1 and #2), which occurred at the ratio f 1.0:0.5. These trends suggest that two or more competing factors are affecting the fracture process.

The point (b) was further evaluated by considering the hypothesis that the *number* of thick film layers was an important factor in the strength and failure mode behavior of these solder joints. In fact, the number of thick film layers corresponded directly to the number of firing steps to which, the LTCC substrate and thick film/LTCC interface were subjected. The pull strength values were plotted as a function of the number of firing steps in Fig. 14. Because there were indications that both strength and failure mode were sensitive

to the pad length distance ratio, only those data for 1.0:1.0 ratios were used to construct Fig. 14.

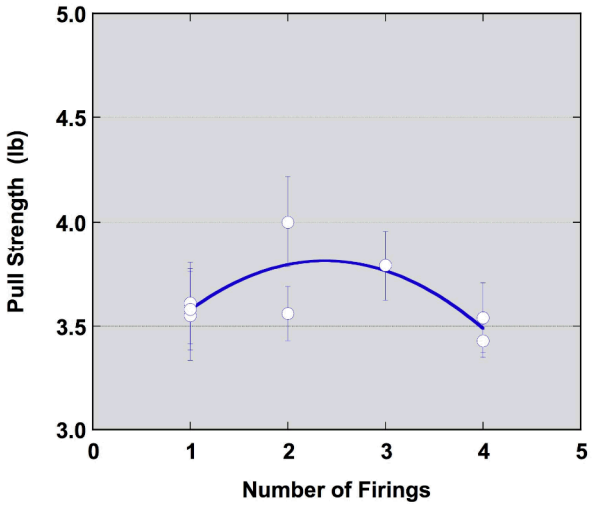

Fig. 14 Pull strength as a function of the number of firings (i.e., thick film layers). The data were included from only those samples having a length distance ratio of 1.0:1.0.

The data points in Fig. 14 suggested that a parabolic trend was present. A least squares curve fit was performed using a second order equation. The curve fit line is shown in Fig. 14. The R^2 value was 0.53, which signified a satisfactory correlation. This analysis indicated that a maximum strength was obtained when there are between two and three *total* number of firing steps. Because the same trend was observed when cases were included that had ratios other than 1.0:1.0 – including similar regression parameters, similar trends and regression correlations – it was concluded that the firing steps dependence transcended the pad geometries factor.

The failure mode data were similarly evaluated as a function of the number of thick film firing steps (layers). Those results are shown in Fig. 15 for modes #1, #3, and #4. The data in Fig. 15, like that in Fig. 14, included, at first, only those cases in which the length distance ratio was 1.0:1.0. Again, as in case of the strength analysis above, the same trends and regression analysis correlations were observed when all of the data were included in the evaluation.

The following observations were compiled from the data in Fig. 15. As the number of firing steps increased, there was a decrease in the mode #1 failures. A linear regression analysis was most appropriate for mode #1 (R^2 = 0.75). In particular, between one and two firing steps, the increase of solder/thick film strength resulted in the fracture path moving into the bulk solder (mode #3). The latter failure mode trend was best represented by a second order, least squares equation (R^2 = 0.82). This trend suggested that there was a strengthening of the solder/thick film interface when going from one firing step and two firing steps, which coincided with the increased pull strength shown in Fig. 14. The "two-firings" case is specific to the 1x 5742, 1x 4596 samples (with and without vias). These results imply that introducing the 1x 5742 between a 1x 4596 layer and the LTCC causes, indirectly, an improvement to the solder/thick film interface strength.

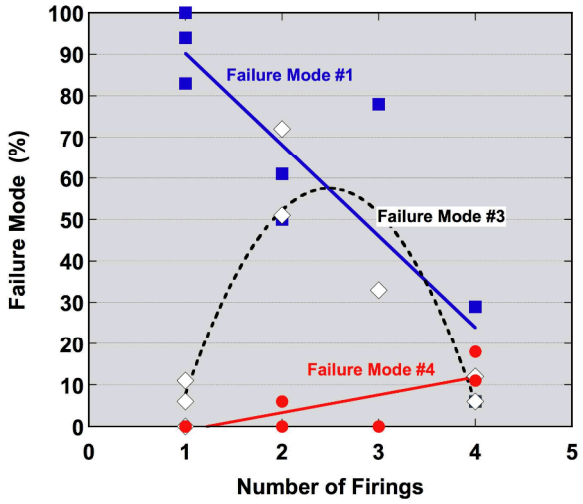

Fig. 15 Failure mode as a function of number of firings (i.e., thick film layers). The data were included from only those samples having a length distance ratio of 1.0:1.0.

Microstructurally, it was difficult to identify a specific mechanism where by, the 5742 barrier to glassy phase movement from out of the 1x 4596 layer, could have indirectly improved solder adhesion to the 1x 4596 thick film surface. It can be stated that the improved adhesion was not due to the number of firing steps because, whether alone or on top of the 1x 5742 layer, the 4596 layer reflects only a *single* firing step. Determining a synergy between the solder/thick film interface and presence of the barrier layer will require further surface analysis of these samples that was beyond the scope of this work.

Referring to Fig. 15, when there were more than two firing steps, there was an increased occurrence of failure mode #4. This trend implied that there was a decrease of the thick film/LTCC interface bond strength. The strength loss of this interface dominated over the solder joint failure mode #3 as evidenced by the latter's rapid decrease. As such, the increased occurrence of thick film/LTCC interface failures accompanied the decrease of overall solder joint pull strength (Fig. 14). Unlike the thick film surface and resulting solder/thick film interface, the thick film/LTCC interface is exposed to *every* firing step. Therefore, the data in Fig. 15 suggested that there was a degradation to that interface and underlying LTCC material (e.g., divots) that resulted when the number of firing steps exceeds 2 – 3.

Results and Discussion – Failure Mode Microstructure

This study also examined the microstructures of the pull-tested samples using metallographic cross section and SEM imaging techniques. As noted above, a quantitative assessment was performed on the failure mode behavior provided by the cross sections; however, those results are not discussed, explicitly, here. Rather, a qualitative summarization is made of those data. Shown in Fig. 16a is an SEM photograph of the pull tested solder joint from a sample

having a 1x 4596 thick film layer without the via. The upward force was applied on the left-hand side of the Cu lead; this position was designated as the *front* of the solder joint. The fracture surface was comprised of failure at the solder/thick film interface for approximately 63% of the bond line, beginning at the front of the joint. A higher magnification image is shown in Fig. 16b (taken at the location of the yellow box in Fig. 16a), which illustrated this failure mode. There was no deformation to the thick film layer. The presence of the 4596 glassy phase is identified in the LTCC substrate. The remainder of the fracture surface towards the back of the joint was along the thick film/LTCC interface. The change of failure mode was not a consequence of the void. Rather, the appearance of this mode was likely a consequence of the greater contribution of shear forces to the to a mixed shear/tensile stress state that resulted from deformation of the Cu lead.

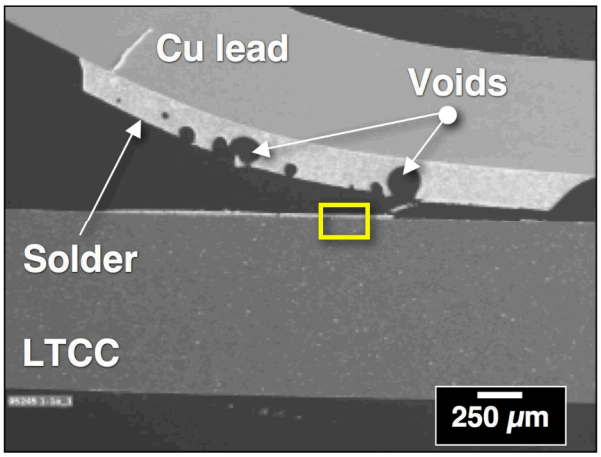

(a)

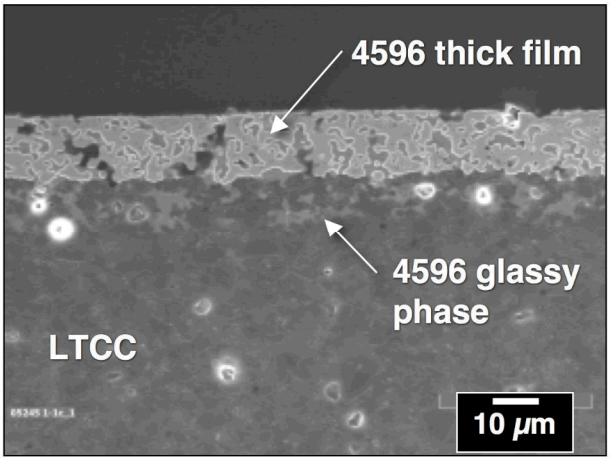

(b)

Fig. 16 SEM photographs showing the pull tested solder joint from a sample having a 1x 4596 layer (no via): (a) low magnification view of the pull tested solder and (b) high magnification view showing the solder/thick film interface separation at the yellow box location in (a).

A second solder joint pull test site provided the opportunity to view a cross section of the thick film/LTCC failure mode. Shown in Fig. 17 are two SEM photographs that correspond to either side of the fracture. This sample had a 1x 4596 layer (no via, as well). The image in Fig. 17a shows no deformation to the thick film. The photograph in Fig. 17b shows that the failure occurred directly at the interface between the metal layer and the glassy phase. There was no evidence of cracking in, or pull-out from, the LTCC substrate.

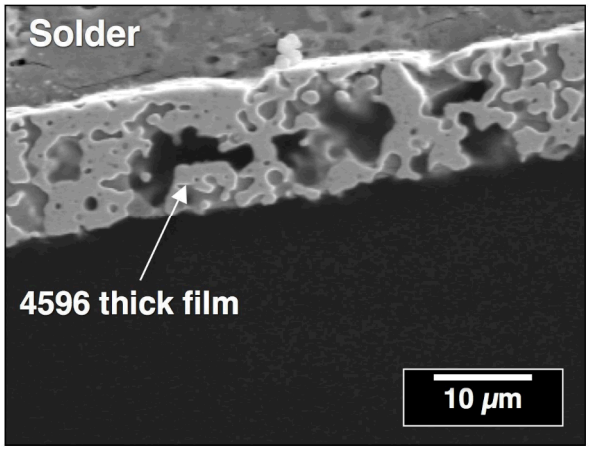

(a)

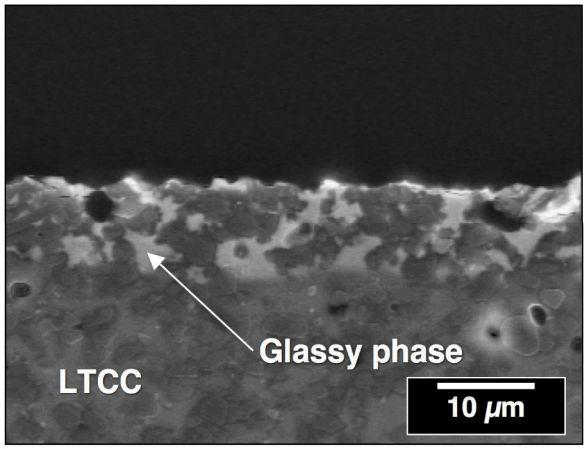

(b)

Fig. 17 SEM photographs showing the corresponding surfaces of a thick film/LTCC failure mode (1x 4596 layer, no via): (a) thick film side and (b) the LTCC side.

The failure mode that was not detected by visual inspection, but could only be observed through the test site cross sections, was fracture within the combined 1x 5742, 3x 4596 layer. This failure mode – termed *bulk thick film failure* – is shown in Fig. 18. The SEM image was taken from the sample having 3x 4596 layer and 1x 5742 (1.0:0.2). The fracture path occurred along the "boundary" of accumulated glassy phase particles (black dotted line) between the two thick film compositions. However, the fracture was highly

ductile as evidenced by voids that were, in fact, created by the cup-and-cone separation.

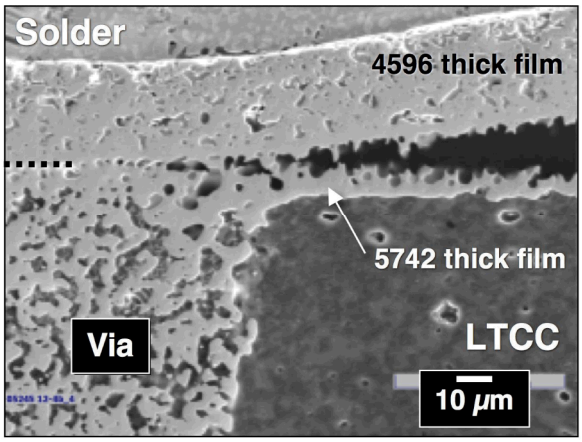

Fig. 18 SEM photograph that shows fracture along the boundary between 1x 5742 and 3x 4596 layer (1.0:0.2).

The bulk thick film failure mode was not very prevalent. It occurred in three sample categories. Two of those categories had the 3x 4596 layer. In these instances, this mode occurred at the back end of the joint. The third case was the very strong, 1x 5742, 1x 4596 sample (no vias) in which the bulk thick film fracture occurred throughout the joint. Therefore, aside from the mixed-mode stress state at the back of the joint, this failure mode was associated with those circumstances in which failure did not take place at the other interfaces.

Although not detected by visual inspection, the 1x 5742 layer (In-Pb, via) samples showed a contribution by the thick film/LTCC failure mode, which is illustrated by Fig. 19.

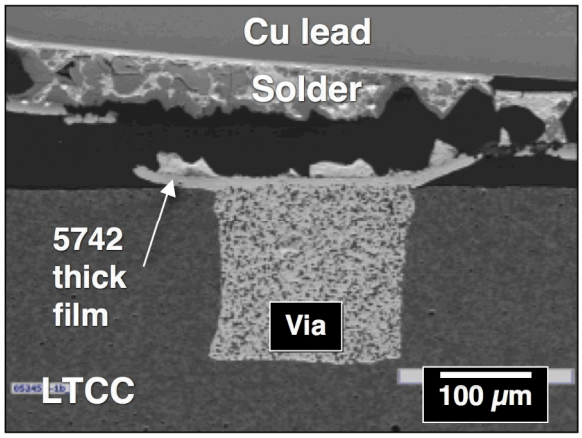

Fig. 19 SEM photograph showing the failure behavior of the 1x 5742 thick film and In-Pb solder interconnection.

Typically, over the via, there is excellent adhesion between the 5742 layer and the via fill, so the fracture path switched to the solder/thick film interface. It was interesting to observe that, when the 1x 5742 layer was combined with either the 1x or 3x 4596 layers, fracture specifically at the 5742/LTCC interface was very rare. If this failure mode was present, it was limited to very small regions of the bond line.

The failure mode analyses of the cross sectioned solder joints provided the following observations:

(a) In the case of the 4596 thick film on LTCC, a larger number of firing steps, i.e., from 1x to 3x, caused the glassy phase to diffuse further into the substrate. However, no general glassy phase diffusion was observed with the 5742 layer. Rather, it was observed in only a few, isolated locations.

(b) The prevalent failure modes of the 1x and 3x 4596 layers directly on LTCC were solder/thick film and thick film/LTCC interface fractures. While the two modes contributed to similar extents for the 1x 4596 layer, the thick film/LTCC mode was observed to a greater degree with the thicker 3x 4596 layer. This trend further substantiated the earlier observation that excessive firing steps (> 2) tended to weaken the thick film/LTCC interface.

(c) The failure of the stand-alone 1x 5742 layer occurred by separation at both the thick film/LTCC and solder/thick film interfaces.

(d) The addition of the 1x 5742 layer between the 4596 layer and LTCC substrate caused an increased preference for the solder/thick film failure mode, more so for 1x 4596 cases than the 3x 4596 layer samples. Therefore, the presence of the 5742 layer improved the overall thick film/LTCC interface strength, albeit, to different degrees. Bulk thick film failures were observed; but, they were limited to very high pull strengths or in the back of the joint that experienced a greater degree of mixed shear and tensile forces.

(e) The LTCC divots occurred at the back of the joint, where there was a greater mixture of both tensile and shear applied stresses. The divots were more frequently observed with the 3x 4596 layer and when the pad length ratio between the 4596 and 5742 layers was the least.

(f) The vias were not damaged during the pull tests. The side wall cracks, when present, did not affect the fracture morphology.

(g) Solder joint voids affected the fracture morphology on a very localized scale. The corresponding artifact was vertical cracks in the thick film layer. The absence of a large-scale role on fracture behavior coincided with their minimal effect on solder joint strength.

These trends, together with the visual observations, clearly show that multiple factors affect the mechanical behavior of the solder joints made to thick film, LTCC substrates. The underlying factors are: (1) LTCC material strength; (2) thick film/LTCC interface adhesion; (3) bulk thick film strength; (4) solder/thick film interface strength; and (5) the bulk solder strength. The role of bulk solder strength must necessarily consider the significant degree of strain hardening exhibited by these alloys. Because the intrinsic strengths of these structures appear to be of a similar magnitude, the failure modes were sensitive to small changes in any one of them as well as synergistic (or "cross term") effects between them –

e.g., the effects of multiple firing steps on both the interfaces. Nevertheless, this study has provided valuable insights into the behaviors of these complex interconnection structures. This information is critical towards understanding and improving the long-term reliability of LTCC products.

Conclusions

1. A study was performed, which examined the pull strength and microstructures of 63Sn-37Pb (wt.%) solder joints made to thick film conductor layers on low-temperature, co-fired ceramic (LTCC) substrates. Specifically, the thick film solder pads were comprised of the Au-Pt-Pd thick film (DuPont™ 4596) and a Au barrier layer (DuPont™ 5742). The latter was introduced to prevent cracking in via side walls. A single layer (1x) of 5742 (Au) and 1x or 3x layers of 4596 (Au-Pt-Pd) were evaluated.
2. The interconnections exhibited excellent solderability and the expected level of voids.
3. Maximum pull strengths were in the range of 3.5 – 4.0 lbs, which were slightly lower than those of comparable tests on alumina but were still within acceptable limits. However, the current data exhibited considerably less scatter.
4. Strength was maximized for those thick film structures made with 2 – 3 firing steps. Both the solder/thick film and thick film/LTCC interface strengths had roles in this trend, thereby affirming the synergism between material, interfaces, and the firing processes.
5. Optimum pull strength was realized for the combined 4596 and 5742 layer (over vias) when the pad length dimension ratio was 1.0:0.5. The strength maximum was accompanied by a minimal occurrence of the thick film/LTCC failure mode.
6. The predominant failure mode sites were: bulk solder; solder/thick film interface; bulk thick film when both 5742 and 4596 layers were present; thick film/LTCC interface; and LTCC divots. In general, low pull strengths were more apt to be associated with failures at the thick film/LTCC interface. Strengthening of the latter interface moved the fracture site to the solder/thick film interface. Bulk solder failure accompanied both of these modes. At very high strengths, bulk thick film fractures were also observed.

Acknowledgments

The authors wish to thank J. Rejent and M. Grazier for performing the pull tests; Alice Kilgo, who prepared the metallographic cross sections; P. Hlava for performing the EPMA; and E. Lopez for his careful review of the manuscript.

References

1. Harper, C., *ed.,* Handbook of Thick film Hybrid Microelectronics, McGraw-Hill (New York, 1982).
2. Holmes, P. and Loasby, R., *eds.* Handbook of Thick Film Technology Electrochem. Pub., Ltd. (Ayr, Scotland, UK, 1976).
3. Hitch, T. and Bube, K., "Baside Adhesion Mechanisms in Thick and Thin Film," RCA Laboratories Report for Naval Air Systems Command PRRL-77-CR-2 RCA Laboratories (New Jersey, 1976).
4. Crossland, W. and Hailes, L., "Thick Film Conductor Adhesion Reliability," *Solid State Tech.,* Vol. 14 (1971) pp. 42 – 47.
5. Perecherla, R. and Buchanan, R., "Adhesion Failure Modes in Copper Thick Film Conductors," *Inter. J. of Microelec. and Elec. Packaging*, Vol. 18, (1995) pp. 29 – 40.
6. Ewsuk, K., Monroe, S., Uribe, F., Morgenstern, H., and Zawicki, L., "Design of a Barrier Layer to Eliminate Cicumferential Cracking in LTCC Packaging," intermal report, Sandia National Laboratories (Albuquerque, NM 2005).
7. DuPont is a registered trademark of the E. I. du Pont de Nemours and Company, Wilmington, DE.
8. "Acceptance Requirements – Thick Film Fritted Conductor Paste", *SS309297 Issue J*, Appendix E. Sandia National Laboratories, Albuquerque, NM.